Monte Carlo simulation and parameterized treatment on the effect of nuclear elastic scattering in high-energy proton radiography [*]

XU Hai-Bo(许海波)   ZHENG Na(郑娜)[1)]

Institute of Applied Physics and Computational Mathematics, Beijing 100094, China

Abstract: A version of Geant4 has been developed to treat high-energy proton radiography. This article presents the results of calculations simulating the effects of nuclear elastic scattering for various test step wedges. Comparisons with experimental data are also presented. The traditional expressions of the transmission should be correct if the angle distribution of the scattering is Gaussian multiple Coulomb scattering. The mean free path (which depends on the collimator angle) and the radiation length are treated as empirical parameters, according to transmission as a function of thickness obtained by simulations. The results can be used in density reconstruction, which depends on the transmission expressions.

Key words: proton radiography, multiple Coulomb scattering, angle collimator, nuclear elastic scattering, Geant4

PACS: 29.27.Eg   **DOI:** 10.1088/1674-1137/39/7/078201

1   Introduction

High-energy proton radiography offers a promising new diagnostic technique to determine the geometric configuration and physical characteristics related to primary implosion phenomena, because the mean free path can be tailored to allow seeing inside almost any experiment [1]. Proton radiography has been shown to be far superior to flash X-ray radiography. In proton radiography, the attenuation of protons passing through an object is measured by focusing the transmitted beam onto an image plane detector with a set of quadrupole magnets. Protons interact with matter by way of the strong and electromagnetic interactions. The three most important effects on the protons as they go through an object are absorption, multiple Coulomb scattering, and energy loss [2–4]. First, some of the protons are absorbed by interacting with nuclei. The absorption of the protons through a given thickness can be expressed as a simple exponential formula. Second, the protons undergo a small change of angle in the proton direction by interacting with the electric fields of nuclei. The phenomenon is called multiple Coulomb scattering (MCS), which causes radiograph blurring because of the angular dispersion, and changes the total attenuation when an angle-cut collimator is placed to make cuts on the MCS angle. Third, protons lose energy by interacting with atomic electrons. This process is well described by the Bethe-Bloch theory. This energy spread causes image blurring due to chromatic aberrations in the magnetic lens.

For full-scale hydrotest experiments or dense materials, a fourth process nuclear elastic scattering, by which protons scatter at some angle by interacting with nuclei can be important for the transmitted angular distribution [5, 6]. In this paper, our simulations clearly show the requirement for inclusion of nuclear elastic scattering in order to agree with experimental results.

The traditional expressions for proton transmission should be correct if the anglular distribution of the scattering is Gaussian MCS. In determining volume density distributions by fitting parametric models of the objects to experimental radiographs, the mean free path, which depends on the collimator angle and the radiation length, is treated as an empirical parameter. In this paper, the net attenuation of the illuminating beamlets by angle-cut collimation will be emphasized.

2   Basic equation of proton radiography

A traditional model for proton radiography can be obtained by assuming a simple exponential formula for nuclear attenuation and the angular distribution of the scattering as Gaussian MCS [1–4, 7–9]. In such a case, the transmission of protons through the magnetic lens and angle-cut collimators at the Fourier plane is de-

scribed by the following form:

$$T(L) = \exp\left(-\sum_i \frac{L_i}{\lambda_i}\right)\left[1 - \exp\left(-\frac{\theta_{\text{cut}}^2}{2\theta_0^2}\right)\right]$$

$$= \exp\left(-\sum_i \frac{L_i}{\lambda_i}\right)\left\{1 - \exp\left[-\kappa\bigg/\left(\sum_i L_i/X_{0i}\right)\right]\right\}. \tag{1}$$

Here, L_i is the areal density for the ith material, and λ_i is the nuclear attenuation factor for the ith material, given by

$$\lambda_i = \frac{A_i}{N_A \sigma_i}, \tag{2}$$

where N_A is Avogadro's number, A_i is the atomic weight and σ_i is the absorption cross section for the ith material. θ_{cut} is the magnitude cut imposed by the angle-cut collimator, and θ_0 is the multiple coulomb scattering angle, given approximately by

$$\theta_0 \approx \frac{14.1\ \text{MeV}}{pc\beta}\sqrt{\sum_i^n \frac{L_i}{X_{0i}}}. \tag{3}$$

Here, p is the beam momentum, $\beta = v/c$ where v is the beam velocity and c is the speed of light, and X_{0i} is the radiation length for the ith material, given by

$$X_{0i} = \frac{716.4 A_i}{Z_i(Z_i+1)\ln\left(287/\sqrt{Z_i}\right)}. \tag{4}$$

The scale κ,

$$\kappa = \frac{1}{2}\left(\frac{pc\beta\theta_{\text{cut}}}{14.1\ \text{MeV}}\right)^2, \tag{5}$$

is independent of L and the material.

The effect of beam emittance on the transmission can be included in this Gaussian approximation by adding the additional contribution to the beam divergence referenced to the offset a, normalized to units of κ, in quadrature to the multiple scattering caused by the object [6, 7]. This gives

$$T(L)$$

$$= \exp\left(-\sum_i \frac{L_i}{\lambda_i}\right)\left[1 - \exp\left(-\frac{\theta_{\text{cut}}^2}{2\theta_0^2}\right)\right]$$

$$= \exp\left(-\sum_i \frac{L_i}{\lambda_i}\right)\left\{1 - \exp\left[-\kappa\bigg/\left(\sum_i L_i/X_{0i} + a\right)\right]\right\}. \tag{6}$$

The relationship between the divergence of the beam θ_{b}, and the parameter a is

$$a = \left(\frac{pc\beta\theta_{\text{b}}}{14.1\ \text{MeV}}\right)^2. \tag{7}$$

3   Simulation of step wedge based on Geant4 toolkit

3.1   Simulation setup

To test the proton radiography concept at higher energies, experiment E955 for the beam of 24 GeV/c protons provided by the Alternating Gradient Synchrotron (AGS) at the Brookhaven National Laboratory involved a series of transmission measurements as a function of material thickness and position on various objects. Based on the experiment, we made detailed simulations, with the components of the simulation setup shown in Fig. 1. The beam is first prepared with a diffuser and matching lens to meet optics requirements. Next the beam is measured by the front detectors just upstream of the object after which it passes through the object being radiographed. The beam extracted from the AGS was focused onto a 1.2 cm-thick tantalum diffuser. The lens consisted of four quadrupoles of diameter 20 cm and length 120 cm, which were configured to form a magnification imaging lens unit. Either of a pair of collimators, 1.2 m long right circular cylinders of tungsten, was located at the Fourier mid-plane of the lens. The collimators approximated multiple-scattering angle acceptance cuts of 6.68 mrad [6]. In order to make comparisons with experimental data, a set of step wedges was radiographed in the simulation with 24 GeV/c and 10^{10} incident protons.
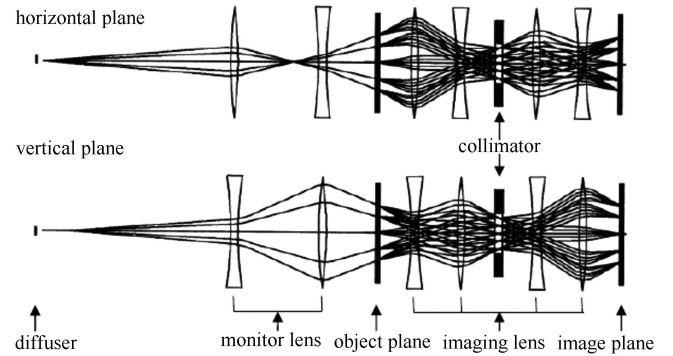

Fig. 1.   Layout of the proton radiography magnetic lens system used for simulation.

3.2   Transmission of the step wedge

Numerical simulation using the Monte Carlo code Geant4 [10] has been implemented to investigate the entire physics mechanism. In the first step, the correct functioning of the Geant4 code is checked by comparing simulation results with measurement results. The calculated results and the experimental results are shown in Figs. 3 and 4. The calculated results and the experimental results are found to be in good agreement.

The central part of the collimator description in the simulation was the same as the experimental set up. Rather than put the object at the object location in Fig.1, there was a mesh tally followed by a minus identity ($-I$) lens (lens 0); the object was centered at the image plane of lens 0, but this collimator did not intercept any protons [11, 12].

These values of transmission versus areal density are plotted in Figs. 2 and 3 for carbon and lead, respectively, where the experimental measurements [13] are also plotted. It should be noted that inclusion of nuclear scattering with the Gaussian MCS would improve the agreement between Monte Carlo simulations and the data.
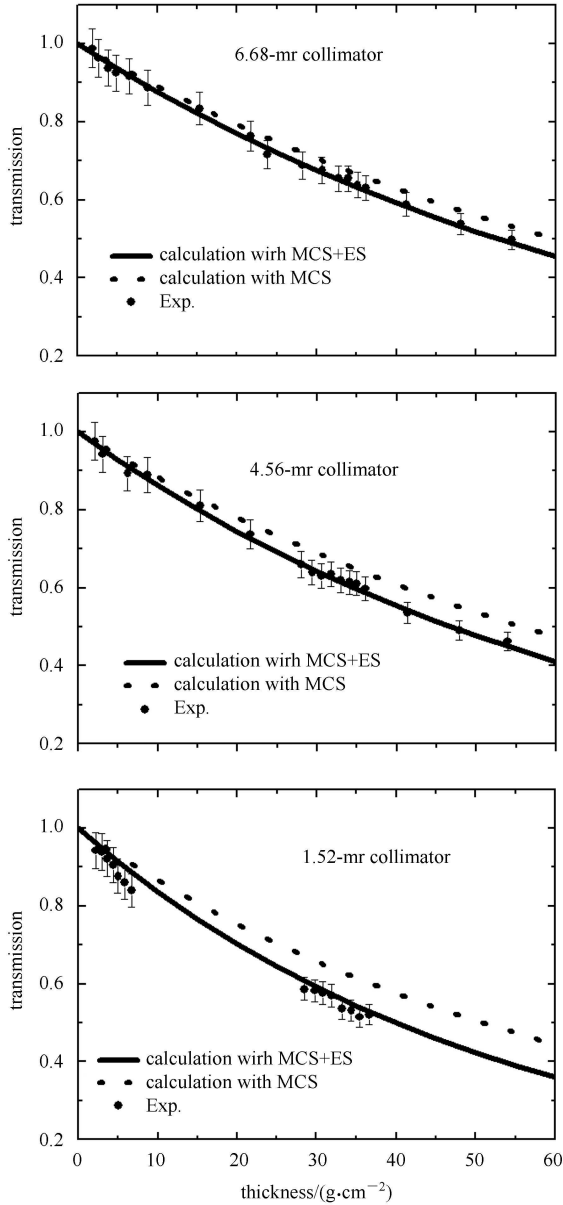

Fig. 2.   Transmissions as a function of thickness for carbon compared with the experiment data for three different angle-cut collimators.
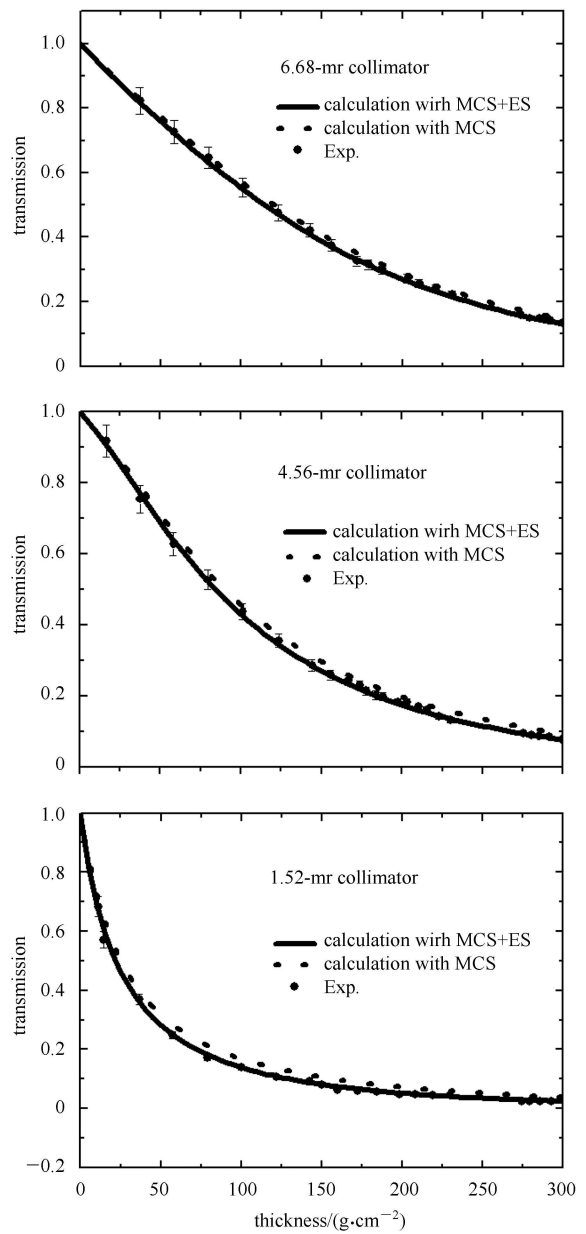

Fig. 3.   Transmissions as a function of thickness for lead compared with the experiment data for three different angle-cut collimators.

4   Parameterized treatment on the effect of nuclear elastic scattering

For thick objects, the angular spread of the beam fraction that passes through the magnetic lens to form the image is dominated by MCS in the radiographed object, but elastic proton–nucleon scattering in the object can also have a significant effect on the transmitted angular distribution. The above expressions should be corrected if the angular distribution of the scattering is

Table 1.   Parameters of the minus identity lens for 24 GeV/c and 50 GeV/c proton radiography.

momentum /(GeV·c^{-1})	quadrupole aperture/mm	quadrupole gradient/(T·m^{-1})	quadrupole length/m	drift length/m	chromatic aberration coefficient/m	field of view/mm
24	120	8	2	3.4	40.4	80
50	220	16.74	3	4	36.1	120

Gaussian MCS. For the step wedge data, the experimental results could not be fit for the three collimators with a given material, with the same values for λ and X_0. In order to fit the data, Morris et al. proposed a method that assumed an angle-cut dependent value of the nuclear interaction length λ for different collimators with one value of X_0 [6]. This result, while possibly functional, was not pleasing because of the addition of new parameters.

Proton radiography requires a high energy beam to penetrate a thick object while keeping the MCS angle and energy loss small enough to allow good spatial resolution. In order to satisfy the goals for quantitative radiography of a dynamic experiment with plutonium, the accelerator design requirement is 50 GeV/c protons for the United States Advanced Hydrotest Facility (AHF). Proton momentum of 50 GeV/c is suitable for the design goal of 1 mm imaging blur. On the other hand, in order to do comparisons with experimental data provided by the AGS at BNL, the nominal proton momentum in E955 was 24 GeV/c.

In this paper, we introduce two scenarios, 24 GeV/c and 50 GeV/c proton radiography beamlines, in which a matching section, the Zumbro lens (minus identity) lens system and imaging system will be particularized. Parameters of the minus identity lens for 24 GeV/c and 50 GeV/c proton radiography are given in Table 1.

Transmission as a function of thickness was obtained by Monte Carlo simulations based on Geant4. Step wedges were imaged to obtain transmission as a function of thickness for eight materials: beryllium, carbon, aluminum, iron, copper, tin, tungsten, and lead. These materials were chosen so that our parameterization would span the periodic table. Results for 24 GeV/c and 50 GeV/c protons are shown in Figs. 4 and 5.

The lines show least-squares fits to the data using Eq. (6). If λ_θ and X_0 are treated as empirical parameters - good fits to transmissions - a function of thickness can be obtained.

In the fit, the X_0 were parameterized by

$$X_0 = \frac{a_x A}{Z(Z+1)\ln\left(b_x/\sqrt{Z}\right)}. \tag{8}$$

The λ_θ were parameterized as

$$\lambda_\theta = a_\theta A^{b_\theta}, \tag{9}$$

for collimator angles θ. Here A and Z are the atomic weight and the atomic number, respectively. The material dependence is entirely contained in the A and Z in Eqs. (8) and (9).

In this fit, the independent parameters are $L_{i,j}$, the areal density of of each step j of the ith material. The dependent parameters are the measured transmissions $T_{i,j}$ through each step. The material properties A_i and Z_i, the beam momentum $p\beta$, and the collimator cut angles θ_{cut} are taken as known constants. This leaves seven parameters to fit: the four collimator-dependent cross section parameters a_θ and b_θ from Eq. (9); the two radiation length parameters a_X and b_X from Eq. (8); and the beam divergence θ_b from Eq. (7).
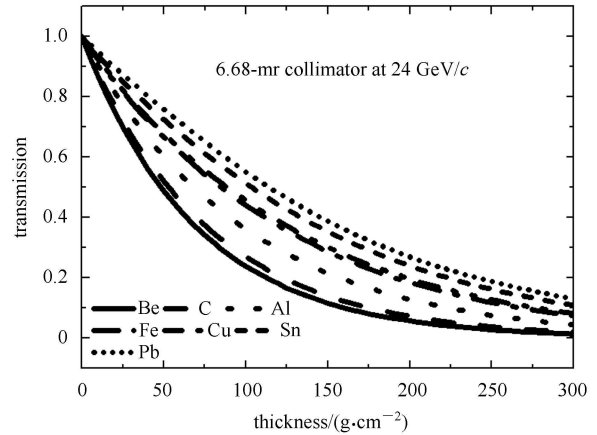

Fig. 4.   The calculated transmissions as a function of thickness for the step wedges data at 24 GeV/c.
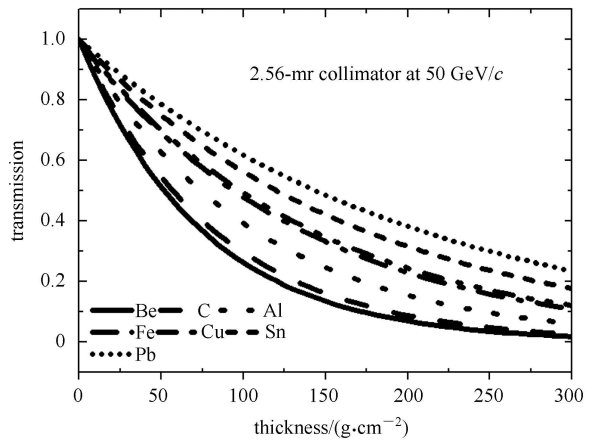

Fig. 5.   The calculated transmissions as a function of thickness for the step wedge data at 50 GeV/c.

Table 2.   Fitted parameters for the radiation length and attenuation length parameterization for 24 GeV/c and 50 GeV/c.

momentum/(GeV/c)		a_θ/(g/cm^2)	b_θ	a_X/(g/cm^2)	b_X	θ_b/mr
24	results from [6]	35.06	0.3182	230.1	34.5	1.05
	our result	34.67	0.3212	228.5	34.8	1.02
50	our result	36.57	0.3260	298.6	38.4	0.93

The fit function can be seen to give a good account of the data over a very wide range in step wedge thickness. In the step wedge fits, below, we will parameterize X_0, and fit for the effective beam emittance θ_b.

For the 24 GeV/c and 50 GeV/c beamline, the results of the fit are given in Table 2. From Table 2, we can see that our results are in good agreement with those in Ref. [6].

Thus, the dependence between the transmissions and thickness (areal density) were obtained for a number of common materials. In the density reconstruction, the transmission radiographs from the experiment and Eq. (6) with the parameters in Table 2 were used to obtain the areal density, and then the Abel inversion was applied to get the volume density from the areal density.

The results for λ approximately follow the expectation based on the geometric model discussed above. The simple geometric model would have given a_θ=37 g/cm^2 and b_θ=1/3 for collimator angles large enough to accept elastic scattering. In our case, the nuclear attenuation length also depends on collimator angle. This is due to the angular dependence of the elastic scattering contribution to the removal cross section.

We note that this parameterization gives radiation lengths X_0 that are significantly different from the standard values, a_X=716.4 g/cm^2 and b_X=287. This may be due to contributions of plural nuclear scattering to the Coulomb multiple scattering distribution, which is not included in the Gaussian approximation used here.

5   Summary

A simulation for proton radiography has been implemented with the Geant4 toolkit. The proper functioning of the Geant4 code and the effects of nuclear elastic scattering for various test step wedges have been checked by comparing simulation results with measurement results provided by AGS at BNL. According to the simulations, the attenuation length parameterization depends on the collimator angle, but the radiation length parameterization is independent of the collimator angle. The fitted parameters do a good job of reconstructing volume density distributions for full-scale hydrotest experiments or thick objects, in which the elastic scattering can also have a significant effect for proton transmission. Further studies related to the volume density reconstruction are currently in progress.

References

1 Amann J F, Espinoza C J, Gomez J J et al. High-Energy Test of Proton Radiography Concepts. Los Alamos National Laboratory, LA-UR-97-1520. 1997
2 King N S P, Ables E, Alrick K R et al. Nuclear Instruments and Methods in Physics Research A, 1999, **424**(1): 84
3 Aufderheide III M B, Park H-S, Hartouni E P et al. Proton Radiography as a Means of Material Characterization. Lawrence Livermore National Laboratory. UCRL-JC-134595. 1999
4 Rigg P A et al. Phys. Rev. B, 2008, **77**: 220101
5 Neri F, Walstrom P L. Nuclear Instruments and Methods in Physics Research B, 2005, **229**: 425
6 Morris C L, Ables E, Alrick K R et al. Journal of Applied Physics, 2011, **109**: 104905
7 XU Hai-Bo. High Power Laser and Particle Beams, 2006, **18**(3): 477–482 (in Chinese)
8 WEI Tao, YANG Guo-Jun, LONG Ji-Dong et al. Chinese Physics C, 2013, **37**(6): 068201
9 Mottershead C T, Zumbro J D. Proceedings of the 1997 Particle Accelerator Conference. Vancouver B C, Canada, 1997, 1397
10 Agostinelliae S, Allisonas J, Amako K et al. Nuclear Instruments and Methods in Physics Research A, 2003, **506**: 250
11 Zumbro J D, Acuff A, Bull J S et al. Radiation Protection Dosimetry, 2005, **117**(4): 447
12 Hughes H G, Brown F B, Bull J S et al. Radiation Protection Dosimetry, 2005, **116**(1–4): 109
13 Zumbro J D, Acuff A, Bull J S et al. Proton Radiography Applications with MCNP Los Alamos National Laboratory. 5LA-UR-04-2997. 2004